Journal of Power Sources 195 (2010) 3293–3299

Contents lists available at ScienceDirect

Journal of Power Sources

journal homepage: www.elsevier.com/locate/jpowsour

Structural and electrochemical properties of the doped spinels $Li_{1.05}M_{0.02}Mn_{1.98}O_{3.98}N_{0.02}$ ($M = Ga^{3+}$, Al^{3+}, or Co^{3+}; $N = S^{2-}$ or F^{-}) for use as cathode material in lithium batteries

Fábio A. Amaral, Nerilso Bocchi*, Ricardo F. Brocenschi, Sonia R. Biaggio, Romeu C. Rocha-Filho

Departamento de Química, Universidade Federal de São Carlos, C.P. 676, 13560-970 São Carlos - SP, Brazil

ARTICLE INFO

Article history:
Received 29 October 2009
Received in revised form
28 November 2009
Accepted 1 December 2009
Available online 4 December 2009

Keywords:
Doped-manganese spinels
Cationic and anionic doping
Mechanical milling
Lithium-ion battery
Cathode material

ABSTRACT

The doped and milled spinels $Li_{1.05}M_{0.02}Mn_{1.98}O_{3.98}N_{0.02}$ ($M = Ga^{3+}$, Al^{3+} or Co^{3+}; $N = S^{2-}$ or F^{-}) are studied aiming at obtaining an improved charge/discharge cycling performance. These spinels are prepared by a solid-state reaction among the precursors ε-MnO_2, LiOH, and the respective oxide/salt of the doping ions at 750 °C for 72 h and milled for 30 min. The obtained spinels are characterized by XRD, SEM, and determinations of the average manganese valence *n*. In the charge and discharge tests, the doped spinels present outstanding initial values of the specific discharge capacity *C* (117–126 mA h g^{-1}), decreasing in the following order: $C(Li_{1.05}Al_{0.02}Mn_{1.98}S_{3.02}O_{3.98}) > C(Li_{1.05}Al_{0.02}Mn_{1.98}F_{3.02}O_{3.98}) > C(Li_{1.05}Ga_{0.02}Mn_{1.98}S_{3.02}O_{3.98}) > C(Li_{1.05}Ga_{0.02}Mn_{1.98}F_{3.02}O_{3.98}) > C(Li_{1.05}Co_{0.02}Mn_{1.98}S_{3.02}O_{3.98}) > C(Li_{1.05}Co_{0.02}Mn_{1.98}F_{3.02}O_{3.98})$. The doped spinel $Li_{1.05}Ga_{0.02}Mn_{1.98}S_{3.02}O_{3.98}$ presents an excellent electrochemical performance, with a low capacity loss even after 300 charge and discharge cycles (from 120 to 115 mA h g^{-1} or 4%).

1. Introduction

In the last decades, the marked increase in the use of portable electronic equipments has been accompanied by the tendency of miniaturization, leading to a demand for batteries of reduced mass and size, but also with long durability, high safety, and low aggression potential to the environment when disposed of [1,2]. Lithium-ion batteries appear as one of the best options to meet the demands of portable electronic equipments, providing the highest energy density values among rechargeable batteries [3,4].

Transition metal sulfides were the first cathodic materials investigated for use in rechargeable lithium batteries, but a significant technological advancement of cathodic materials only occurred [5,6] after the synthesis of $LiCoO_2$ by Mizushima et al. [7]. Since then, metal oxides of transition metals of the first series have been especially attractive as cathodic materials, because they are strong oxidizing agents that facilitate the occurrence of lithium-ion insertion [8]. The lamellar-structure oxides ($LiNiO_2$ and $LiCoO_2$), oxides of inverse-structure spinels ($LiNiVO_4$ and $LiCoVO_4$), and the lithium manganate ($Li_xMn_2O_4$) with spinel structure are among the oxides commonly used in lithium-ion batteries, which operate in the potential ranges 3.5–4.2, 3.5–4.5, and 3.0–4.2 V *vs.* Li/Li^+, respectively [9].

The use of the $Li_xMn_2O_4$ spinel as cathode material in lithium-ion batteries presents some advantages such as: manganese abundance, non-toxicity, low cost, and possibility of insertion of two lithium ions per unit formula. This last aspect is very interesting as lithium-ion batteries can operate either at 4 or 3 V *vs.* Li/Li^+ [10,11]. However, the main disadvantage of using the $Li_xMn_2O_4$ spinel as cathode material is the decrease of the specific capacity during cycling of the lithium-ion battery, specially at temperatures higher than 40 °C, at which most electronic equipment operate [12]. This capacity loss is associated with the lithium-ion extraction/insertion processes into/out of the $Li_xMn_2O_4$ ($0 \le x \le 2$) spinel during successive charge and discharge cycles, respectively. The $Li_xMn_2O_4$ spinel structure possesses three-dimensional interstitial spaces through which lithium ions migrate during extraction/insertion processes. For $0 \le x \le 1$, these processes occur at 4 V *vs.* Li/Li^+ and the cathode cycling can be considered satisfactory because the spinel compact cubic structure formed by O^{2-} ions contracts and expands isotropically during the lithium-ion extraction/insertion processes [11]. On the other hand, for $1 \le x \le 2$, at close to 3 V *vs.* Li/Li^+ lithium ions are inserted into the spinel structure by a reaction that involves two distinct phases [13]. This reaction corresponds to the beginning of an anisotropic distortion

* Corresponding author. Tel.: +55 16 33518079; fax: +55 16 33518350.
E-mail address: bocchi@dq.ufscar.br (N. Bocchi).

0378-7753/$ – see front matter © 2009 Elsevier B.V. All rights reserved.
doi:10.1016/j.jpowsour.2009.12.002

of the $LiMn_2O_4$ compact cubic symmetry to a tetragonal symmetry, known as the Jahn–Teller distortion [11,13–16]. This local distortion is related to the vacancy/occupancy of the e_g antibonding orbital of the Mn^{3+} ion during successive charge and discharge cycles, respectively.

In addition to the Jahn–Teller distortion, several other phenomena have also been pointed out as responsible for the capacity loss of $Li_xMn_2O_4$ spinels, such as: electrolyte degradation at high potentials (>4.4 V *vs.* Li/Li^+); slow dissolution caused by the $2Mn^{3+}(s) \rightarrow Mn^{4+}(s) + Mn^{2+}(slv)$ disproportionation reaction [15,17–21]; instability of the delithiated structure (at the end of the charging process) due to oxygen loss by the spinel structure [18,22]. Thus, various experimental strategies have been carried out in order to minimize such problems of the $Li_xMn_2O_4$ spinels. Among them, the following are worth noting: change of the precursors and synthesis conditions during the spinel preparation by a solid-state reaction [23,24]; use of a spinel with a low excess of lithium ions ($Li_{1.05}Mn_2O_4$) [25,26]; use of different methodologies for spinel synthesis, such as the mechanochemical synthesis [27], polymeric-precursors method (Pecchini) [28], combustion reaction [29,30], and sol–gel method [31]; change of the morphology and size of the spinel particles [32]; introduction of structural defects in the spinel, such as cationic vacancies [33]; deposition of an aluminum film on the surface of the $LiMn_2O_4$ spinel [34]; doping of the spinel with different metallic ions [19,35–39]. Among these strategies, doping of the spinel with small amounts of cations for substituting the Mn^{3+} ions (responsible for the Jahn–Teller effect) seems to be promising in order to obtain spinel cathodes with longer useful life during successive charge and discharge cycles [40]. Accordingly, many researchers have considered doping the $LiMn_2O_4$ spinel with small amounts of usually trivalent ions, such as Cr^{3+}, Co^{3+}, Ga^{3+}, Fe^{3+}, Bi^{3+}, etc. [20,35,37,41–47].

Although cationic doping increases the performance of spinel cathodes at room temperature, they still present significant specific capacity loss at temperatures above 40 °C. This has been attributed to the presence of acidic species from the electrolyte, which cause a slow dissolution of superficial particles of the spinel cathodes [21]. Hence, in order to minimize both effects (Jahn–Teller and dissolution of manganate particles), some authors have proposed concomitant cationic and anionic (S^{2-} or F^-) doping of these spinels [31,48–58].

As mentioned before, the introduction of structural defects in the crystalline network and the control of particle size may also contribute to the maintenance of the specific capacity of spinel cathodes. In this way, mechanical milling of doped spinels (with cations and anions) becomes an alternative low-cost method for introducing structural defects into crystalline networks [57]. Moreover, the use of this methodology, before or after the calcination of the spinel precursors, allows better control of size distribution and particle shape, as well as metal distribution in the host matrix [59]. For this, mechanical milling, combined or not with heat treatment at moderate temperatures, has been used by many authors to obtain electrodic materials [27,60–66].

In a previous work [67] we showed that the $Li_{1.05}Mn_2O_4$ spinel could be easily obtained by a solid-state reaction from ε-MnO_2 (with more structural defects than the γ-form), using only one heating step in the thermal treatment. In this work we report results attained by doping this spinel with cation–anion pairs, obtaining the $Li_{1.05}M_{0.02}Mn_{1.98}O_{3.98}N_{0.02}$ (M = Ga^{3+}, Al^{3+} or Co^{3+}; N = S^{2-} or F^-) spinels. Aiming at improving the capacity performances of these doped spinels, they were obtained by a solid-state reaction between the precursors ε-MnO_2, LiOH, and the respective oxide/salt of the doping ions (Co^{3+}, Ga^{3+}, Al^{3+}, S^{2-}, and/or F^-) at 750 °C for 72 h. In order to control the particle size, the spinels were milled in a ball mill for 30 min.

2. Experimental

2.1. Synthesis of the doped spinels

The following precursors were used in the synthesis of the doped spinels $Li_{1.05}M_{0.02}Mn_{1.98}O_{3.98}N_{0.02}$ (M = Ga^{3+}, Al^{3+} or Co^{3+}; N = S^{2-} or F^-): ε-MnO_2 (prepared as described elsewhere [68]), LiOH (Riedel), Ga_2O_3 (Aldrich), Al_2O_3 (Aldrich), cobalt acetate (Merck), Li_2S (Aldrich), and LiF (Aldrich). The doped spinels were prepared by a solid-state reaction among the precursors in the mole ratios $1.00(Mn_{1.98} + M_{0.02})$:1.05Li and $1.00(O_{3.98} + N_{0.02})$:1.05Li. After homogenization in a mortar, the precursor mixture was calcined in a tubular oven under static air at 750 °C for 72 h and then slowly cooled at a rate of −10 °C min^{-1}. A mixer mill (Spex Certiprep 8000 M) was used for milling all the doped spinels for 30 min.

2.2. Characterization of the spinels

All doped spinels were characterized by XRD, using an automated diffractometer (Siemens D-5000) with Cu Kα radiation and a graphite monochromator; a scan rate of 2° min^{-1} was employed in all measurements.

The morphology and average particle size of the doped spinels were also characterized by SEM, using a Zeiss (DSM 960) microscope.

The average manganese valence in the doped spinels was determined by the Vetter and Jaeger's method [69], in which redox titrations involving the MnO_4^-/Mn^{2+}, Fe^{3+}/Fe^{2+}, and Mn^{3+}/Mn^{2+} redox couples are carried out.

2.3. Electrochemical evaluations

Composite electrodes were prepared by mixing the respective doped spinel with 10% carbon black (Vulcan XC 72-6P 2800, Cabot) and 5% of polyvinylidene fluoride (PVDF) (Aldrich) in cyclopentanone (Aldrich). After this mixture was converted to a viscous and homogeneous paste by using an ultrasonic bath, this paste was applied on a Pt current collector (10 mm × 3 mm × 0.4 mm). All composite electrodes were thermo-pressed at 3.45 MPa and 130 °C for 20 min and then kept under vacuum at 80 °C for 24 h.

For initial charge and discharge tests, a three-electrode glass cell and a potentiostat/galvanostat (EG&G Parc 263A) controlled by appropriate software were employed. The composite electrodes were used as working electrodes, while Li wires (Aldrich) were used as reference and counter electrodes; 1 mol L^{-1} $LiClO_4$ (Aldrich) dissolved in a 2:1 (v/v) mixture of ethylene carbonate (EC) (Aldrich; 98%) and dimethyl carbonate (DMC) (Aldrich) was used as electrolyte. The initial charge and discharge tests were carried out at a constant current density (51 and 102 μA cm^{-2}, respectively) over the potential range 4.35–3.30 V *vs.* Li/Li^+.

For long cycling studies, a Teflon Swagelok-type cell and a thin film of polymeric gel electrolyte were employed. This polymeric gel was prepared from the copolymer poly(acrylonitrile)/poly(vinyl acetate) (PAN/PVA, M = 140,000 g mol^{-1}, Radicy Crylor), containing 93.6% acrylonitrile, 6.1% vinyl acetate, and 0.3% sodium methylsulfonate. For the polymeric gel preparation, $LiBF_4$ (Aldrich) was firstly dissolved in a 2:1 (v/v) EC-DMC mixture at room temperature. Then, the PAN/PVA copolymer was added and dispersed in the mixture, so that the mole percentages of PAN/PVA:2EC:DMC:$LiBF_4$ were 20:35:37:8. The resultant slurry was heated up to 90 °C and kept at this temperature for a short time to promote a fast and complete dissolution. In order to favor gel formation, the resulting solution was slowly cooled to room temperature. Finally, a thin film (~0.5 mm) of the polymeric gel electrolyte was obtained using a film extensor; discs of 10-mm diameter were then cut for use in the cycling cell. The complete details on the preparation of this

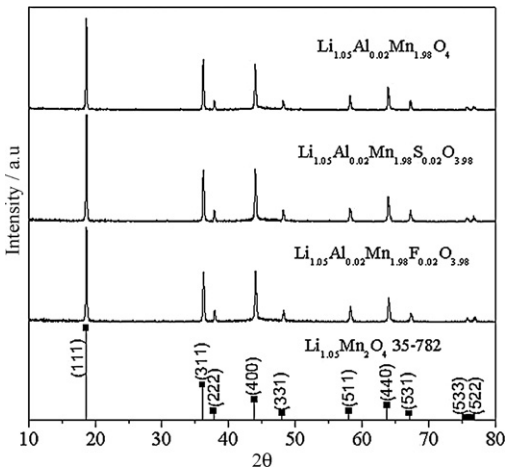

Fig. 1. Typical X-ray diffractograms obtained for the doped spinels $Li_{1.05}Al_{0.02}Mn_{1.98}O_4$, $Li_{1.05}Al_{0.02}Mn_{1.98}S_{0.02}O_{3.98}$, and $Li_{1.05}Al_{0.02}Mn_{1.98}F_{0.02}O_{3.98}$; the diffractogram for the $LiMn_2O_4$ spinel from JCPDS (35-782) is also presented.

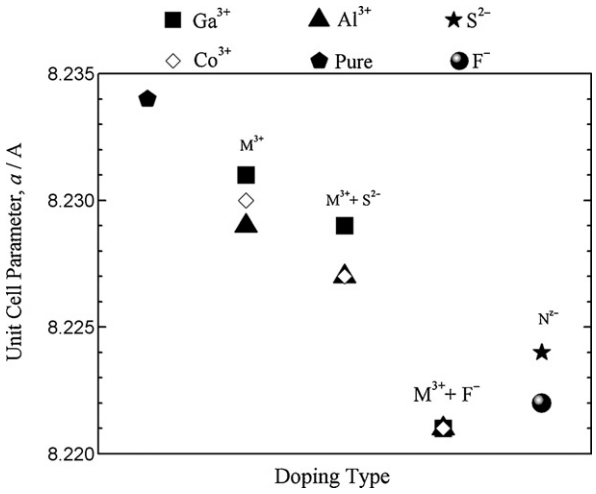

Fig. 2. Values of the unit-cell parameter a calculated for the pure spinel and for the doped spinels $Li_{1.05}M_{0.02}Mn_{1.98}O_{4-z}N_z$ (M = Al^{3+}, Co^{3+}, or Ga^{3+}; z = 0 and 0.02; N = S^{2-} or F^-).

polymeric gel electrolyte are described elsewhere [70]. The long cycling tests were carried out in the same experimental conditions as the initial tests.

All manipulations of air-sensitive materials as well as assemblies were carried out inside a glove box (Labconco 50600), from which humidity was continuously removed through a drying-train accessory. All the obtained measurements using the glass cell were performed inside this box.

3. Results and discussion

Typical X-ray diffractograms obtained for the doped spinels $Li_{1.05}Al_{0.02}Mn_{1.98}O_{3.98}N_{0.02}$ (N = S^{2-} or F^-) are shown in Fig. 1. The well-defined peaks of these diffractograms agree well with those from the JCPDS 35-782 card (also shown in Fig. 1) corresponding to the stoichiometric spinel $LiMn_2O_4$ with a cubic unit cell and *Fd*3*m* space group; no other LiMnO phase or impurity was detected, as also observed by other authors [19,22,48,71]. According to Manev et al. [72] and Lee et al. [73] the position and full width at half maximum (FWHM) of the (4 0 0)-plane peak are important factors indicating the degree of crystallinity of a spinel powder. Manev et al. [72] also pointed out that the mean lithium content in spinels occurs when the (4 0 0) plane is located at $2\theta = 43.95^\circ$ and the FWHM value is 0.1. Table 1 presents the positions and FWHM values of the (4 0 0)-plane peak extracted from the X-ray diffractograms for all doped spinels synthesized in this work. As it can be seen in Table 1, only the Al-doped spinels present positions and FWHM values for the (4 0 0)-plane peak close to those mentioned above. Therefore, among the obtained doped spinels, the Al-doped ones showed the highest degree of crystallinity. Concerning the lithium content, it is expected that the lithium insertion into the doped spinels decrease in the following order: aluminum, gallium, and cobalt. In fact, this is confirmed, as it will be further demonstrated below through the charge and discharge tests. Moreover, Lee et al. [73] also observed that Al-doped spinels with intensity ratio of the (3 1 1)/(4 0 0)-planes peaks in the range of 0.96–1.1 showed good cycling performance. As most of the obtained doped spinels present values of such ratio in this range (see Table 1), one may expect that they will present good cycling performances.

In order to evaluate the influence of the nature of the doping ions on the crystalline lattice of the obtained spinels, the values of the unit-cell parameter a (see Table 1 and Fig. 2) were also calculated from the XRD data by the least-squares method. Table 1 and Fig. 2 also contain the a value (8.234 Å) calculated for the pure spinel obtained at 750 °C for 72 h; from this value it can be inferred that the composition of the pure spinel is very close to that of the stoichiometric $LiMn_2O_4$ spinel from the JCPDS 35-782 card (a = 8.241 Å). Amatucci et al. [52] reported a value of a of 8.235 Å for $Li_xMn_2O_4$ (x = 1.03) obtained by a solid-state reaction at 800 °C for 24 h. As it can be seen in Fig. 2, the values of a calculated for all the doped spinels were always lower than that for the pure one, suggesting an effective doping since this process is associated with the substitution of Mn^{3+} ions (ionic radius of 0.65 Å) in octahedral (16d) sites by cations of the same oxidation state and smaller ionic radius (Al^{3+}, Co^{3+}, or Ga^{3+} with ionic radius of 0.53, 0.60, or 0.63 Å, respectively) [74]. For cationic doping, as the respective ionic radius decreases the value of a decreases in the same order: a($Li_{1.05}Ga_{0.02}$

Table 1
Values of the position and FWHM for the (4 0 0)-plane peak, intensity ratio of the (3 1 1)/(4 0 0)-planes peaks, unit-cell parameter, and average manganese valence for all the doped spinels.

Spinel	Plane (4 0 0)/degree		Ratio of the (3 1 1)/(4 0 0) planes	Unit-cell parameter† a/Å	Average manganese valence n
	Position/2θ	FWHM			
$Li_{1.05}Al_{0.02}Mn_{1.98}O_4$	43.94	0.22	1.1	8.229	3.56 ± 0.01
$Li_{1.05}Al_{0.02}Mn_{1.98}S_{0.02}O_{3.98}$	43.96	0.24	0.97	8.227	3.57 ± 0.01
$Li_{1.05}Al_{0.02}Mn_{1.98}F_{0.02}O_{3.98}$	43.96	0.26	0.97	8.221	3.57 ± 0.01
$Li_{1.05}Ga_{0.02}Mn_{1.98}O_4$	44.00	0.24	1.1	8.231	3.60 ± 0.01
$Li_{1.05}Ga_{0.02}Mn_{1.98}S_{0.02}O_{3.98}$	44.05	0.26	0.97	8.229	3.59 ± 0.01
$Li_{1.05}Ga_{0.02}Mn_{1.98}F_{0.02}O_{3.98}$	44.05	0.28	0.97	8.221	3.59 ± 0.01
$Li_{1.05}Co_{0.02}Mn_{1.98}O_4$	44.10	0.24	1.2	8.230	3.58 ± 0.01
$Li_{1.05}Co_{0.02}Mn_{1.98}S_{0.02}O_{3.98}$	44.14	0.29	0.95	8.227	3.57 ± 0.01
$Li_{1.05}Co_{0.02}Mn_{1.98}F_{0.02}O_{3.98}$	44.16	0.32	0.93	8.221	3.58 ± 0.01

† a = 8.234 Å for the pure spinel obtained at 750 °C for 72 h.

$Mn_{1.98}O_4$) > a($Li_{1.05}Co_{0.02}Mn_{1.98}O_4$) > a($Li_{1.05}Al_{0.02}Mn_{1.98}O_4$). For cationic and anionic doping, the value of a decreases in the following order: a(spinel doped with M^{3+}) > a(spinel doped with M^{3+} and S^{2-}) > a(spinel doped with M^{3+} and F^-). Although three different cations were used, the values of a were also affected by the value of the ionic radius of the anion S^{2-}(1.84 Å) or F^-(1.33 Å). However, this analysis does not explain the values of a calculated for the spinels doped only with S^{2-}, whose ionic radius is greater than that of O^{2-}(1.60 Å). In this case, the greater electronic affinity of S^{2-} may possibly explain the smaller value of a obtained for the spinel doped with only S^{2-}. The bond-energy values for the O^{2-} anion in the spinel lattice may also explain the values of a for the spinels doped only with anions, as the value of that physical quantity is greater for S^{2-}–O^{2-} and F^-–O^{2-} than for O^{2-}–O^{2-}. In general, the values of a calculated for all doped spinels in the present work agree well with those reported in the literature [13,20,51,54,75].

As in the case of the values of a, the values of the average manganese valence n are also important in order to evaluate the doping of spinel samples, since a decrease in the values of a might usually occur due to an increase in the manganese oxidation state [76]. The values of n for the doped spinels are always greater than that for the pure one (Fig. 3); this is in agreement with the values of a calculated for all the doped spinels. Therefore, the values of both a and n are indicative of the effective doping of the spinels. Among the spinels doped only with cations,

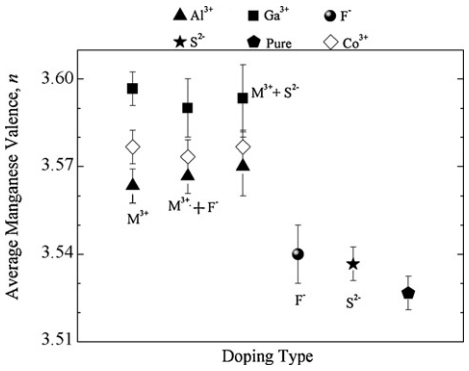

Fig. 3. Values of the average manganese valence n determined for the pure spinel and for the doped spinels $Li_{1.05}M_{0.02}Mn_{1.98}O_{4-z}N_z$ (M = Al^{3+}, Co^{3+}, or Ga^{3+}; z = 0 and 0.02; N = S^{2-} or F^-); the bars indicate the average standard deviations for at least three determinations.

the values of n decrease in the following order: n($Li_{1.05}Ga_{0.02}Mn_{1.98}O_4$) > n($Li_{1.05}Co_{0.02}Mn_{1.98}O_4$) > n($Li_{1.05}Al_{0.02}Mn_{1.98}O_4$). On the other hand, the anionic doping practically does not change the values of n. Some dispersion in the values of n was also observed by other authors and can be attributed to the presence of either stoichiometric defects or small amounts of other phases not detectable by XRD [77].

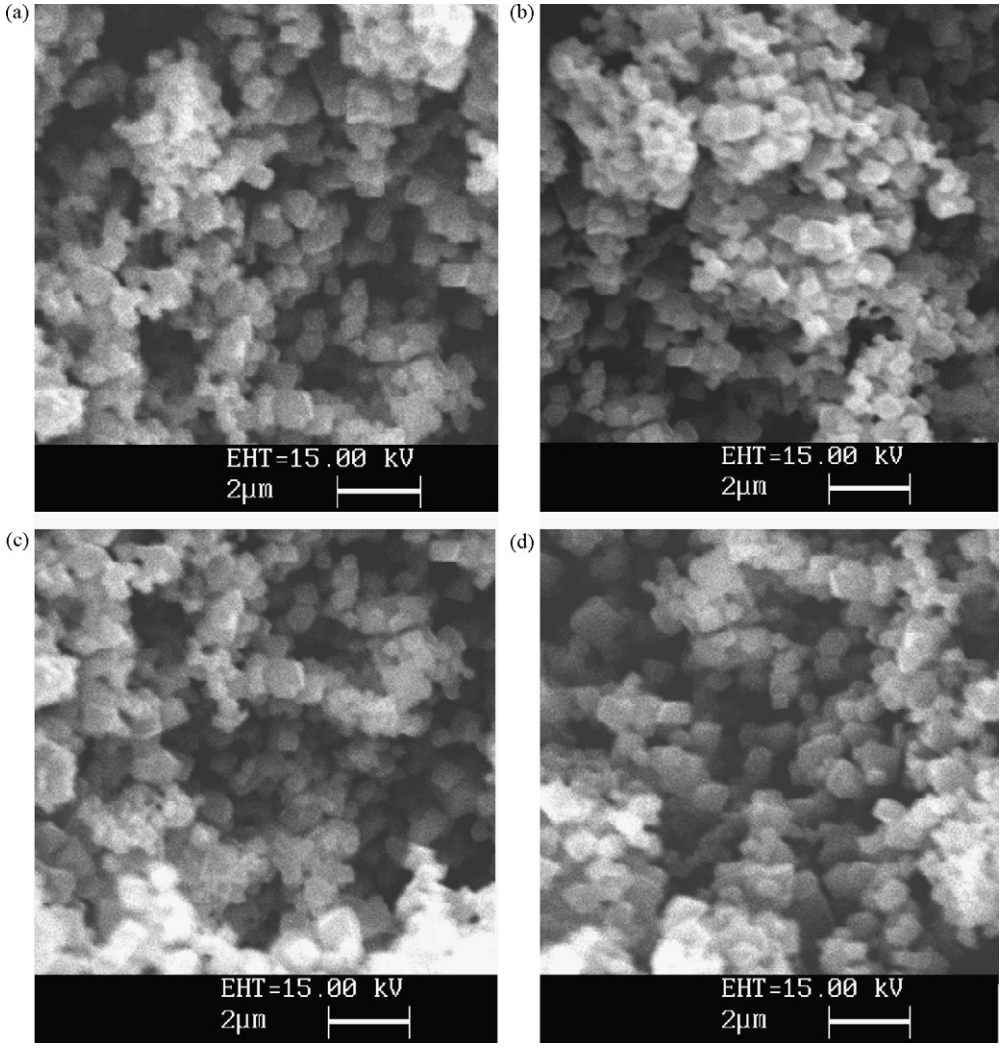

Fig. 4. Typical SEM micrographs for the following doped spinels: (a) $Li_{1.05}Al_{0.02}Mn_{1.98}O_4$; (b) $Li_{1.05}Ga_{0.02}Mn_{1.98}O_4$; (c) $Li_{1.05}Co_{0.02}Mn_{1.98}O_4$; (d) $Li_{1.05}Mn_2S_{0.02}O_{3.98}$.

Since the surface morphology is also an important factor for the cycling performance, that was also examined by SEM for all the doped spinels investigated in this work. Thus, Fig. 4 illustrates typical SEM micrographs obtained for four different doped spinels; similar images were obtained for the other spinels. In all cases, grains of similar forms and uniform size distribution are observed. The average grain size is less than 400 nm. In general, the surface morphology of the doped spinels is quite similar to those observed by other authors [49,75,78,79].

Before the cycling studies, cathodes prepared from all the spinels (pure and doped) were firstly submitted to initial charge and discharge tests over the potential range 4.35–3.30 V *vs.* Li/Li^+. After the tenth cycle, all spinels presented values of the specific capacity 5–15% higher than that observed for the pure spinel ($\sim$110 mA h g^{-1}) obtained only by calcination (without further milling) [67]. These results are possibly related to a more uniform particle size distribution after the milling of the spinel. However, for milling times higher than 30 min the values of the specific capacity decreased significantly due to the formation of other new phases, confirmed by XRD (not shown). This is why all the spinels in the present work were milled in a ball mill for 30 min. As the values of specific capacity were practically maintained during the initial charge and discharge tests, cathodes prepared from all the doped spinels investigated in this work were submitted to long cycling tests. The values of specific capacity obtained during 300 charge and discharge cycles for cathodes prepared from all the doped spinels investigated in this work in a PAN/PVA-based gel electrolyte are presented in Fig. 5. Clearly, the spinel concomitantly doped with Al^{3+} and S^{2-} presented the highest values of specific capacity while the spinel concomitantly doped with Ga^{3+} and S^{2-} presented the lowest value of capacity loss (4%) after 300 charge and discharge cycles. As shown in Table 2, this last result is among the best ones reported in the literature in the last decade for cycling performance (initial capacity and its retention) of doped-manganese spinels prepared by distinct methodologies. On the other hand, the spinel concomitantly doped with Co^{3+} and F^- showed the lowest specific capacity values and also the worst maintenance of these values. Nevertheless, it is worth pointing out that, even for this last doped spinel, the capacity loss was only 8%, confirming the excellent performance of the cathodes prepared from all the doped spinels.

It is important to point out again that all the doped spinels were submitted to a milling process in order to control their particle size. Comparing the values of the initial specific capacity obtained for the doped spinels (Fig. 5) with that obtained for the pure spinel without further milling ($\sim$105 mA h g^{-1}), one observes that the former are approximately 10% higher. Therefore, both the doping (cationic and anionic) and the milling processes contributed to increase the specific capacity and to maintain its value during the cycling of the spinels. The increase in the specific capacity values is possibly related to a better distribution of particles and their smaller

Table 2
Main results of cycling performance (initial capacity and its retention) of doped-manganese spinels prepared by distinct methodologies, reported in the literature in the last decade.

Researchers	Material	Synthesis	Initial capacity (mA h g^{-1})	Number of cycles	Capacity loss
Pistoia et al. [35]	$Li_{1+x}M_yMn_{2-(x+y)}O_{4+2}$ (M = Li, Cu, Zn, Ni, Co, Fe, Cr, Ga, Al, B, or Ti)	Solid-state reaction at 730 °C for 72 h	~100	150	~7%
Zhang et al. [43]	$LiCr_xMn_{2-x}O_4$ ($0 \le x \le 0.1$)	Solid-state reaction at 600 °C for 15 h and 650 °C for 48 h with intermittent grinding	118 ($x = 0.1$)	200	6.7%
Arora et al. [41]	$LiCo_yMn_{2-y}O_4$ ($0 \le y \le 0.33$)	Solid-state reaction at 600 °C for 6 h and 750 °C for 72 h with intermittent grinding	100	85	2–3%
Wang et al. [44]	$LiCr_xMn_{2-x}O_4$ ($x = 0$, 0.04, 0.06 or 0.1)	Pechini method	122 ($x = 0.04$)	50	7%
Lee et al. [46]	$LiM_{0.05}Mn_{1.95}O_4$ (M = Li, B, Al, Co or Ni)	Citrate–gel method	125 (Ni-doped)	110	2%
Sun et al. [54]	$LiAl_{0.24}Mn_{1.76}O_{3.98}S_{0.02}$	Sol–gel method	109 104 99 144 ($x = 0$)	50 50 50 50	1% at 25 °C 3% at 50 °C 5% at 80 °C 17% at 25 and 45 °C
Myung et al. [53]	$LiAl_xMn_{2-x}O_4$ ($0 \le x \le 0.6$)	Emulsion-drying method	114 ($x = 0.2$)	50	4% at 45 °C
Amatucci et al. [52]	$LiAl_x Mn_{2-x}O_{4-z}F_z$ ($x = 0.1$ or 0.2; $0 \le z \le 0.5$)	Solid-state reaction at 800 °C for 24 h	~100 ($x = 0.2$; $z = 0.5$)	400	15% at 55 °C
Sun et al. [56]	$LiAl_{0.18}Mn_{1.82}O_{3.97}S_{0.03}$	Sol–gel method	107 100	50 50	3% at 25 and 50 °C 7% at 80 °C
Sun et al. [57]	$LiNi_{0.5}Mn_{1.5}O_{4-x}S_x$ ($x = 0$ or 0.05)	Co-precipitation at 500 °C and 800 °C	122 ($x = 0.05$; 500 °C)	50	4%
Wu et al. [49]	$LiMn_{1.5}Ni_{0.5-x}Co_xO_4$ ($0 \le x \le 0.5$)	Spray-drying method	112 ($x = 0.2$)	20	1.8%
Yi et al. [22]	$LiAl_{0.05}Mn_{1.95}O_4$	Adipic acid-assisted sol–gel method at 800 °C	128 ($D_{50} = 17.3$ pm)	50	8.3%
Liu et al. [75]	$LiGa_xMn_{2-x}O_4$ ($0 \le x \le 0.05$)	Sol–gel method	118 ($x = 0.05$)	50	9%
Li and Xu [34]	$LiMn_2O_4$	Solid-state reaction at 600 °C for 6 h and 750 °C for 72 h with intermittent grinding	112	200	6.5%
Zhou et al. [20]	$Ag_x/LiMn_2O_4$ ($0 \le x \le 0.3$)	Thermal decomposition	95 ($x = 0.2$)	40	3.3%
Patoux et al. [42]	$LiNi_{0.4}Mn_{1.6}O_4$	Solid-state reaction at 600–900 °C for 10 h	129	1000	20%
Luo et al. [48]	$LiMn_{1.8}Li_{0.1}Ni_{0.1}O_{4-n}F_n$ ($n = 0$, 0.1 or 0.15)	Solid-state reaction at 450 °C for 12h	80 ($n = 0$)	50	~1%
Huang et al. [47]	$LiM_xMn_{2-x}O_{4-y}Br_y$ ($0 \le x \le 0.15$; $0 \le y \le 0.05$)	Solid-state coordination at 700 °C for 10h	104 ($x = 0.15$; $y = 0.05$)	100	14.5%

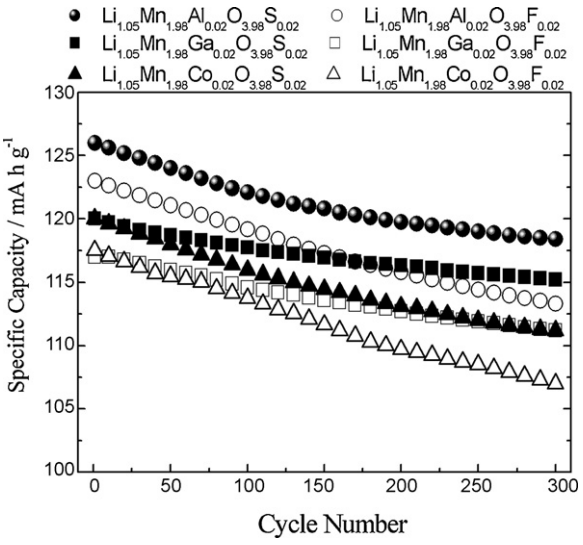

Fig. 5. Specific capacity as a function of cycle number obtained during charge and discharge tests for cathodes prepared from the different doped spinels $Li_{1.05}M_{0.02}Mn_{1.98}O_{3.98}N_{0.02}$ (M = Ga^{3+}, Al^{3+}, or Co^{3+}; N = S^{2-} or F^{-}) using a PAN/PVA-based gel electrolyte; j_c = 51 μA cm^{-2} and j_d = 102 μA cm^{-2}.

size, occupation of sites previously unoccupied, and increase of the spinel porosity. On the other hand, the maintenance of the specific capacity values throughout the cycling process is possibly related to lower volumetric variation of the spinel's unit cell and decreased content of Mn^{3+} ions that are responsible for the Jahn–Teller effect in the uncharged spinels.

4. Conclusions

The solid-state reaction among the precursors ε-MnO_2, LiOH, and the respective oxide/salt of the doping ions (Co^{3+}, Ga^{3+}, Al^{3+}, S^{2-} and F^{-}) at 750 °C for 72 h yielded high quality (no by-products detected) and well-defined doped spinels $Li_{1.05}M_{0.02}Mn_{1.98}O_{3.98}N_{0.02}$ (M = Ga^{3+}, Al^{3+} or Co^{3+}; N = S^{2-} or F^{-}). The mechanical milling of the doped spinels in a ball mill for 30 min yielded a uniform particle size distribution, with an average particle size of less than 400 nm. The values of the unit-cell parameter *a* calculated for all the doped spinels (8.221–8.229 Å) were always lower than that for the pure one (8.234 Å), decreasing in the following order: $a(Li_{1.05}Ga_{0.02}Mn_{1.98}O_4) > a(Li_{1.05}Co_{0.02}Mn_{1.98}O_4) > a(Li_{1.05}Al_{0.02}Mn_{1.98}O_4) > a(Li_{1.05}M_{0.02}Mn_{1.98}O_{3.98}S_{0.02}) > a(Li_{1.05}M_{0.02}Mn_{1.98}O_{3.98}F_{0.02})$. The values of the average manganese valence *n* for the doped spinels (3.56–3.50) were higher than that for the pure spinel (3.53 ± 0.01), decreasing in the following order: $n(Li_{1.05}Ga_{0.02}Mn_{1.98}O_4) > n(Li_{1.05}Co_{0.02}Mn_{1.98}O_4) > n(Li_{1.05}Al_{0.02}Mn_{1.98}O_4) > n(Li_{1.05}M_{0.02}Mn_{1.98}O_{3.98}F_{0.02}) > n(Li_{1.05}M_{0.02}Mn_{1.98}O_{3.98}S_{0.02})$. In the charge and discharge tests, the cathodes of the doped spinels presented values of the specific discharge capacity *C* decreasing in the following order: $C(Li_{1.05}Al_{0.02}Mn_{1.98}S_{3.02}O_{3.98}) > C(Li_{1.05}Al_{0.02}Mn_{1.98}F_{3.02}O_{3.98}) > C(Li_{1.05}Ga_{0.02}Mn_{1.98}S_{3.02}O_{3.98}) > C(Li_{1.05}Ga_{0.02}Mn_{1.98}F_{3.02}O_{3.98}) > C(Li_{1.05}Co_{0.02}Mn_{1.98}S_{3.02}O_{3.98}) > C(Li_{1.05}Co_{0.02}Mn_{1.98}F_{3.02}O_{3.98})$. Although the $Li_{1.05}Al_{0.02}Mn_{1.98}S_{3.02}O_{3.98}$ cathode presented the highest initial capacity (126 mA h g^{-1}), the $Li_{1.05}Ga_{0.02}Mn_{1.98}S_{3.02}O_{3.98}$ cathode presented the smallest capacity loss (from 120 to 115 mA h g^{-1} or 4%) after 300 charge and discharge cycles; this outstanding result is among the best ones reported in the literature for doped-manganese spinels. Therefore, both the doping (cationic and anionic) and the milling processes contributed to obtain much improved cathode materials. Besides presenting an increased specific capacity, the obtained cathodes maintained its value almost constant even after extensive cycling.

Acknowledgements

The authors gratefully acknowledge the Brazilian-funding agencies CNPq, CAPES, and FAPESP for scholarships and financial support for this work.

References

[1] B. Scrosati, Nature 75 (1998) 271.
[2] A. Manthiram, in: G.-A. Nazri, G. Pistoia (Eds.), Lithium Batteries – Science and Technology, Springer, New York, 2009, pp. 3–41.
[3] S. Hossain, in: D. Linden (Ed.), Handbook of Batteries, McGraw-Hill, New York, 1995, pp. 36–77.
[4] F.G. Will, J. Power Sources 63 (1997) 582.
[5] S.C. Canobre, L. Montanhez, C.P. Fonseca, S. Neves, Mater. Chem. Phys. 114 (2009) 350.
[6] B. Ammundsen, in: G.-A. Nazri, G. Pistoia (Eds.), Lithium Batteries – Science and Technology, Springer, New York, 2009, pp. 361–380.
[7] K. Mizushima, P.C. Jones, P.J. Goodenaugh, Mater. Res. Bull. 15 (1980) 783.
[8] M. Broussely, B. Biensan, B. Simon, Electrochim. Acta 45 (1999) 3.
[9] G. Delmas, L. Ménétrier, L. Croguennec, S. Levasseur, J.P. Pérès, C. Pouillerie, G. Prado, L. Fournès, F.L. Weill, Int. J. Inorg. Mater. 1 (1999) 315.
[10] M.M. Thackeray, A. De Kock, M.H. Rossouw, W. Liles, D.R.E. Bittihn, D. Hoge, J. Electrochem. Soc. 139 (1992) 363.
[11] D. Guyomard, J.M. Tarascon, Solid State Ionics 69 (1994) 222.
[12] Y. Gao, J.R. Dahn, J. Electrochem. Soc. 143 (1996) 1783.
[13] K.M. Shaju, P.G. Bruce, Chem. Mater. 20 (2008) 5557.
[14] D.M. Levi, K. Gamolsky, D. Aurbach, U. Heider, R. Oesten, J. Electrochem. Soc. 147 (2000) 25.
[15] Y.K. Sun, B. Oh, J.H. Lee, Electrochim. Acta 46 (2000) 541.
[16] C.M. Julien, Solid State Ionics 177 (2006) 11.
[17] D.H. Jang, Y.J. Shin, S.M. Oh, J. Electrochem. Soc. 143 (1996) 2204.
[18] R.J. Gummow, A. Derock, M.M. Thackeray, Solid State Ionics 69 (1994) 59.
[19] C.P. Fonseca, M.A. Bellei, F.A. Amaral, S.C. Canobre, S. Neves, Energy Convers. Manage. 50 (2009) 1556.
[20] W.J. Zhou, B.L. He, H.L. Li, Mater. Res. Bull. 43 (2008) 2285.
[21] J. Cho, M.M. Thackeray, J. Electrochem. Soc. 146 (1999) 3577.
[22] T.F. Yi, D.L. Wang, K. Gao, X.G. Hu, Rare Met. 26 (2007) 330.
[23] J.M. Marilla, J.L. Martín De Vidales, R.M. Rojas, Solid State Ionics 127 (2000) 73.
[24] J.M. Tarascon, W.R. Mckinmon, F. Coowar, T.N. Bowmer, G. Amatucci, D. Guyomard, J. Electrochem. Soc. 141 (1994) 1421.
[25] R.J. Gummow, A. Dekock, M.M. Thackeray, Solid State Ionics 69 (1994) 59.
[26] D. Song, H. Ikuta, T. Uchida, M. Wakihara, Solid State Ionics 117 (1999) 151.
[27] N.V. Kosova, R.T. Uvarov, Solid State Ionics 135 (2000) 107.
[28] W. Liu, F. Chaput, B. Dunn, G.C. Farrington, J. Electrochem. Soc. 143 (1996) 879.
[29] E.I. Santiago, S.T. Amarcio-Filho, P.R. Bueno, L.O.S. Bulhões, J. Power Sources 97–98 (2001) 447.
[30] C.P. Fonseca, T.T. Cezare, S. Neves, J. Power Sources 112 (2002) 395.
[31] Y.K. Sun, Y.S. Jeon, Electrochem. Commun. 1 (1999) 597.
[32] G. Pistoia, G. Wang, Solid State Ionics 66 (1993) 135.
[33] J. Schoonman, H.L. Tuller, E.M. Kelder, J. Power Sources 81–82 (1999) 44.
[34] X. Li, Y. Xu, Electrochem. Commun. 9 (2007) 2023.
[35] G. Pistoia, A. Antonini, R. Rosati, C. Bellitto, G.M. Ingo, Chem. Mater. 9 (1997) 1443.
[36] M. Wohlfahrt-Mehrens, A. Butz, R. Oesten, G. Arnold, R.P. Hemmer, R.A. Huggins, J. Power Sources 68 (1997) 582.
[37] A. De Kock, E. Ferg, R.J. Gummow, J. Power Sources 70 (1998) 247.
[38] M.M. Sharma, B. Krishnan, S. Zachariah, C.U. Shah, J. Power Sources 79 (1999) 69.
[39] C. Vogler, A. Butz, H. Dittrich, G. Arnold, M. Wohlfahrt-Mehrens, J. Power Sources 84 (1999) 243.
[40] L.S. Kanevskii, V.S. Dubasova, Russ. J. Electrochem. Soc. 41 (2005) 1.
[41] P. Arora, B.N. Popov, R.E. White, J. Electrochem. Soc. 145 (1998) 807.
[42] S. Patoux, L. Daniel, C. Bourbon, H. Lignier, C. Pagano, F. Le Cras, S. Jouanneau, S. Martinet, J. Power Sources 189 (2009) 344.
[43] D. Zhang, B.N. Popov, R.E. White, J. Power Sources 76 (1998) 81.
[44] G.X. Wang, D.H. Bradhurst, H.K. Liu, S.X. Dou, Solid State Ionics 120 (1999) 95.
[45] D. Zhang, B.N. Popov, Y.M. Podrazhanky, P. Arora, R.E. White, J. Power Sources 83 (1999) 121.
[46] J.H. Lee, J.K. Hong, D.H. Jang, Y.K. Sun, S.M. Oh, J. Power Sources 89 (2000) 7.
[47] Y. Huang, R. Jiang, S.J. Bao, Z. Dong, Y. Cao, D. Jia, Z. Guo, J. Solid State Electrochem. 13 (2009) 799.
[48] Q. Luo, T. Muraliganth, A. Manthiram, Solid State Ionics 180 (2009) 703.
[49] H.M. Wu, J.P. Tu, Y.F. Yuan, J.Y. Xiang, X.T. Chen, X.B. Zhao, G.S. Cao, J. Electroanal. Chem. 608 (2007) 8.
[50] Y.K. Sun, Y.S. Jeon, H. Lee, Electrochem. Solid-State Lett. 3 (2000) 7.
[51] P.S. Whitfield, I.J. Davidson, J. Electrochem. Soc. 147 (2000) 4476.
[52] G. Amatucci, N. Pereira, T. Zheng, J.M. Tarascon, J. Electrochem. Soc. 148 (2001) A171.
[53] S.T. Myung, S. Komaba, N.J. Kumaga, J. Electrochem. Soc. 148 (2001) A482.
[54] Y. Sun, G. Park, Y. Lee, M. Yoashio, J. Electrochem. Soc. 148 (2001) A994.
[55] Y.K. Sun, K.S. Nahm, Korean J. Chem. Eng. 19 (2002) 718.
[56] Y.K. Sun, Y.S. Lee, M. Yoshio, Mater. Lett. 56 (2002) 418.

[57] Y.K. Sun, S.W. Oh, C.S. Yoon, H.J. Bang, J. Prakash, J. Power Sources 161 (2006) 19.
[58] L. Wang, L. Jiangang, H. Xiangming, P. Weihua, W. Chonrong, J. Changyin, J. Solid State Electrochem. 13 (2009) 1157.
[59] C. Suryanarayana, Prog. Mater. Sci. 46 (2001) 1.
[60] Y. Sato, T. Nakano, K. Kobayakawa, T. Kawai, A. Yokoyama, J. Power Sources 75 (1998) 271.
[61] G.X. Wang, S. Zhong, D.H. Bradhurst, S.X. Dou, H.K. Liu, J. Power Sources 76 (1998) 141.
[62] N.V. Kosova, I.P. Asanov, E.T. Devyatkina, E.G. Avvakumov, J. Solid State Chem. 146 (1999) 184.
[63] F.R. Hu, Z.D. Peng, J.H. Yang, G.H. Shou, Y.X. Liu, Trans. Nonferrous Met. Soc. China 10 (2000) 817.
[64] N.V. Kosova, E.T. Devyatkina, S.G. Kozlova, J. Power Sources 97–98 (2001) 406.
[65] W.T. Jeong, K.S. Lee, J. Power Sources 104 (2002) 195.
[66] T.W. Jeong, J.H. Joo, K.S. Lee, J. Alloys Compd. 358 (2003) 294.
[67] L.C. Ferracin, F.A. Amaral, N. Bocchi, Solid State Ionics 130 (2000) 215.
[68] E.A. Laurindo, F.A. Amaral, M.L. dos Santos, L.C. Ferracin, A. Carubelli, N. Bocchi, R.C. Rocha-Filho, Química Nova 22 (1999) 600.
[69] K.J. Vetter, N. Jaeger, Electrochim. Acta 11 (1966) 401.
[70] F.A. Amaral, C. Dalmolin, S.C. Canobre, N. Bocchi, S.R. Biaggio, R.C. Rocha-Filho, J. Power Sources 164 (2007) 379.
[71] T. Okumara, T. Fukutsuka, Y. Uchimoto, N. Sakai, K. Yamaji, H. Yokokawa, J. Power Sources 189 (2009) 643.
[72] V. Manev, T. Faulkner, J. Engel, Proc. HBC98, The First Hawaii Battery Conference, 1998, p. 228.
[73] Y.S. Lee, N.J. Kumada, M. Yoshio, J. Power Sources 96 (2001) 376.
[74] R.D. Shannon, Acta Crystallogr. 32 (1976) 751.
[75] D.Q. Liu, Z.Z. He, X.Q. Liu, J. Alloys Compd. 440 (2007) 69.
[76] M.R. Palacín, G.G. Amatucci, M. Anne, Y. Chabre, L. Seguin, P. Strobel, J.M. Tarascon, G. Vaughan, J. Power Sources 89 (2000) 7.
[77] F. Lecras, P. Strobel, M. Anne, D. Bloch, J.B. Soupart, J. Rousche, Eur. J. Solid State Inorg. Chem. 33 (1996) 67.
[78] C.H. Han, Y.S. Hong, H.S. Hong, K. Kim, J. Power Sources 111 (2002) 176.
[79] S.H. Kang, J.B. Goodenough, L.K. Raberberg, Chem. Mater. 13 (2001) 1758.